of the weighting function, eq 10. The error is at its highest at $x = 0$ due to the little weight given to this end when $k \geq 0$.

Conclusion

Within the framework of the present weighting function the generally most reliable results are obtained for *n*-paraffins by the b1 ($k = 0$) approximation; for the complete spectra the error is −2.5% for C_1 and −1.5% for C_3 and falls below 1% beyond C_3 while, for the out-of-plane spectra, the error ranges from −3.1% for C_3 to −2.7% for C_{14}. Other types of approximations which give better results for a particular spectrum are predictable on the basis of the absolute error curves.

Acknowledgment. We gratefully acknowledge use of computer time at the Computer Center of the State University of New York at Stony Brook.

Supplementary Material Available: Two tables of typical results of the approximations for the ZPE's of *n*-paraffins (2 pages). Ordering information is given on any current masthead page.

Potential Surface Walking and Reaction Paths for C_{2v} Be + H_2 ← BeH_2 → Be + 2H ($^1A_1$)

Douglas O'Neal, Hugh Taylor, and Jack Simons*

Department of Chemistry, University of Utah, Salt Lake City, Utah 84112 *(Received: June 20, 1983)*

By combining the surface walking algorithm of Simons et al. with locally determined forces on an ab initio surface, the reaction paths for the model reactions Be + H_2 ← BeH_2 → Be + 2H ($^1A_1$) were studied. This represents the first application of this algorithm to an ab initio surface which is generated locally as the walking proceeds.

Introduction

The development of ab initio molecular gradient techniques[1-6] has made it much more feasible to examine theoretically the energetics of chemical reactions. In fact, it may even now be practical to use these methods within dynamical studies of molecular reactivity. Analytical expressions for molecular gradients (forces) and Hessians (force constant matrices) allow one to avoid tedious and inefficient finite difference calculations and provide efficient tools to use in locating both stable molecular geometries and reaction transition states. Stable molecular geometries have gradient components along all molecular distortions equal to zero and all Hessian eigenvalues (local-normal-mode frequencies) positive. Transition states have vanishing gradients and Hessians with only one negative eigenvalue.

When combined with an efficient surface walking procedure,[7,8] ab initio analytical gradients can be used to proceed, on a single potential energy surface, from a reactant geometry, along various deformation directions, to transition-state geometries and onward to the product molecules. Simons et al.[7] have recently developed and implemented, within the context of globally known two- and three-dimensional model potential energy surfaces, such an algorithm which we now utilize for the first time in an ab initio study where the surface is not globally known but is actually generated as the walk proceeds.

The model reactions

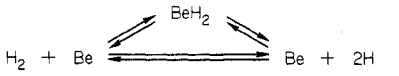

occur on the same ($^1A_1$) potential energy surface in C_{2v} symmetry. The two product states (Be + 2H and BeH_2) arise through a bifurcation of the Be + H_2 reaction path (defined below) which occurs after the transition state has been surmounted. In the present work the reaction Be + H_2 → BeH + H is eliminated from consideration since the molecular deformations are (arbitrarily and artificially) restricted to retain C_{2v} symmetry. For this reason, we must consider our reaction study to be of a modelistic nature. It does, however, represent the first ab initio application of the surface walking algorithm of ref 7 to a locally generated energy surface which contains branching.

The local description of the potential energy surface generated via our walk-driven ab initio quantum-chemical calculations also contains information about the forces and curvatures transverse to the direction of the reaction path. In a future work, we plan to make use of this information to carry out a dynamical study of the above reactions of Be + H_2 utilizing generalizations of the reaction path Hamiltonian method of Adams, Handy, and Miller.[9] We are particularly interested in developing an improvement of the reaction path dynamics method of ref 9 to permit the incorporation of channel branching.

The Surface Walking Algorithm

To efficiently utilize local force and curvature information, the dependence of the electronic energy E on each of the molecule's n internal distortion coordinates $\{X_i; i = 1, 2, ..., n\} = \mathbf{X}$ is Taylor series expanded[7] about the geometry[10] $\mathbf{X} = \mathbf{0}$

$$E(\mathbf{X}) - E(\mathbf{0}) \simeq \sum_i F_i X_i + \tfrac{1}{2}\sum_{i,j} X_i H_{ij} X_j \qquad (1)$$

(1) P. Pulay in "Modern Theoretical Chemistry", H. F. Schaefer III, Ed., Plenum Press, New York, 1977, Chapter 4.
(2) J. D. Goddard, N. C. Handy, and H. F. Schaefer III, *J. Chem. Phys.*, **71**, 1525 (1979); Y. Osamura, Y. Yamaguchi, and H. F. Schaefer III, *ibid.*, **75**, 2919 (1981); **77**, 383 (1982); B. R. Brooks, W. D. Laidig, P. Saxe, J. D. Goddard, Y. Yamaguchi, and H. F. Schaefer III, *ibid.*, **72**, 4652 (1980).
(3) J. A. Pople, R. Krishnan, H. B. Schlegel, and J. S. Brinkley, *Int. J. Quantum Chem.*, **13**, 225 (1979); R. Krishnan, H. B. Schlegel, and J. A. Pople, *J. Chem. Phys.*, **72**, 4654 (1980).
(4) H. F. King and M. Dupuis, *J. Comput. Phys.*, **21**, 1 (1976); M. Dupuis, J. Rys, and H. F. King, *J. Chem. Phys.*, **65**, 111 (1976); M. Dupuis and H. F. King, *ibid.*, **68**, 3998 (1978).
(5) A. Komornicki, K. Ishida, K. Morokuma, R. Ditchfield, and M. Conrad, *Chem. Phys. Lett.*, **45**, 595 (1977); K. Ishida, K. Morokuma, and A. Komormichi, *J. Chem. Phys.*, **66**, 2153 (1977).
(6) P. Jørgensen and J. Simons, *J. Chem. Phys.*, in press.
(7) J. Simons, P. Jørgensen, H. Taylor, and J. Ozment, *J. Phys. Chem.*, **87**, 2745, (1983).
(8) C. J. Cerjan and W. M. Miller, *J. Chem. Phys.*, **75**, 2800 (1981).
(9) J. E. Adams, N. C. Handy, and W. H. Miller, *J. Chem. Phys.*, **72**, 99 (1980).

0022-3654/84/2088-1510$01.50/0

Here, F_i is the energy gradient (force) along X_i and H_{ij} in an element of the Hessian (curvature) matrix. In the calculations on Be + H_2 reported later in this paper, the Hessian matrix $\boldsymbol{H}$ is obtained either through applying finite-difference methods to the force vector $\mathbf{F}$ or by using update techniques[11] to generate $\boldsymbol{H}$ at a new geometry from knowledge of $\mathbf{F}$ and $\boldsymbol{H}$ at a preceding geometry and $\mathbf{F}$ at the new geometry. Such approximations to $\boldsymbol{H}$ were employed because analytical ab initio expressions[6] for $\boldsymbol{H}$ have not yet been implemented for multiconfigurational (MC) wave functions such as the reactions of Be + H_2 require.

Given a local $\mathbf{F}$ and $\boldsymbol{H}$, one could consider making stationary the quadratic approximation given in eq 1. However, the resultant (Newton–Raphson) prediction for the step ($\mathbf{X}$)

$$\mathbf{X}_{NR} = -\boldsymbol{H}^{-1}\mathbf{F} \tag{2}$$

is not generally appropriate to take. To see why, we substitute $\mathbf{X}_{NR}$ into eq 1 to obtain the predicted energy change which accompanies this step:

$$E(\boldsymbol{X}_{NR}) - E(\mathbf{0}) \simeq -\tfrac{1}{2}\mathbf{F}\boldsymbol{H}^{-1}\mathbf{F} = -\tfrac{1}{2}\sum_a F_a^2 b_a^{-1} \tag{3}$$

The last identity above occurs when $\boldsymbol{H}$ and $\mathbf{F}$ are expressed in the basis in which the Hessian is diagonal:

$$\boldsymbol{H}\mathbf{V}_a = b_a\mathbf{V}_a \tag{4}$$

$$\mathbf{F}\cdot\mathbf{V}_a \equiv F_a \tag{5}$$

Clearly, the Newton–Raphson (NR) step gives rise to an energy change along the $\mathbf{V}_a$ mode whose sign is opposite that of b_a. When one is near an equilibrium molecular structure and one desires to walk "downhill" in energy to a local minimum, the NR step probably makes sense because the local-curvature eigenvalues $\{b_a\}$ are all likely to be positive. The NR step then leads (eq 3) to energy lowering along all modes. Also, when in the neighborhood of a transition state, one of the b_a (say b_1) is negative and the others ($0 < b_2 < b_3 < b_4 < \ldots$) are positive. The NR step then leads to an energy increase along the b_1 mode and energy decreases along the transverse modes. Again the NR step seems entirely reasonable and can, in fact, be correct in these cases.

However, if one is near an equilibrium molecular structure and desires to move *away* from this geometry and toward a transition state, the NR step direction is disasterous. Likewise, to move away from the neighborhood of a transition state and toward a stable-molecule geometry, the NR step is inappropriate. In ref 7 Simons et al. showed how to systematically walk "uphill" along any local normal-mode direction in a manner which is designed to minimize the energy along all modes transverse to the uphill walking direction.[12] Such a stream bed walk procedure was used successfully in ref 7 on several model potential surfaces. By considering the stationary points of the energy function of eq 1 subject to a constrained (fixed) total step length[13] $\mathbf{X}\cdot\mathbf{X} = h^2$, the algorithm of ref 7 produces the step vector

$$\mathbf{X} = (\lambda\boldsymbol{I} - \boldsymbol{H})^{-1}\mathbf{F} = \sum_a (\lambda - b_a)^{-1}F_a\mathbf{V}_a \tag{6}$$

(10) This geometry ($\mathbf{X} = 0$) represents the current position in the stepwise walking algorithm being outlined here.

(11) R. Fletcher, "Practical Methods of Optimization", Vol. 1, Wiley, New York, 1980.

(12) This walking strategy in which the energy is minimized in $n - 1$ directions and maximized (i.e., by moving uphill) along one direction generates what ref 9 calls a reaction path. As in the case for the BeH_2 example treated here, a potential energy hypersurface may have more than one reaction path. To systematically search for possible transition states, one must therefore explore such stream bed walks starting along all possible local-normal-mode directions of the reactant molecule.

(13) In ref 7 a procedure for automatically updating the value of the step length (h) was introduced. This procedure is based upon comparing the energy change predicted by eq 3 to the actual energy change experienced once the step of eq 6 is taken. If these two energy changes agree well, then h is increased; if they differ substantially, h is decreased. In the present work, we simply used a reasonably small constant step length because we wanted to generate a rather smooth reaction path rather than to move to the transition state in as few steps as possible.

TABLE I: Contracted Gaussian Basis Used for BeH_2

		exp	contraction coeff
Be	1s	1267.07	0.001 940
		190.356	0.014 786
		43.2959	0.071 795
		12.1442	0.236 348
		3.809 23	0.471 763
		1.268 47	0.355 183
	1s′	5.693 880	−0.028 876
		1.555 630	−0.177 565
		0.171 855	1.071 630
	1s″	0.057 181	1.000 000
	2p	5.693 880	0.004 386
		1.555 630	0.144 045
		0.171 855	0.949 692
H	1s	19.2406	0.032 828
		2.8992	0.231 208
		0.6534	0.817 238
	1s′	0.177 60	1.000 000

which, when substituted into eq 3, gives a predicted energy change of

$$E(\mathbf{X}) - E(\mathbf{0}) = \sum_{a=1}^{n} \frac{F_a^2}{(\lambda - b_a)^2}(\lambda - \tfrac{1}{2}b_a) \tag{7}$$

As shown in ref 7, the Lagrange multiplier λ is chosen to make the total step length obey $\mathbf{X}\cdot\mathbf{X} = h^2$. However, this condition

$$h^2 = \sum_a \frac{F_a^2}{(\lambda - b_a)^2} \tag{8}$$

does not have a unique solution; as many as $2n$ solutions may exist (see ref 7 for details). When $\lambda < b_1 < b_2 < \ldots < b_n$, the energy change of eq 7 is negative along all n eigendirection, but when $b_1 < \lambda < {}^1/_2 b_2$, it is positive (uphill) along the $\mathbf{V}_1$ direction and negative along all transverse directions. It is precisely this range $b_1 < \lambda\ {}^1/_2 b_2$ in which λ should be chosen so as to generate a stream bed walk which is uphill along the $\mathbf{V}_1$ direction and which remains in or near the stream bed (minimum-energy geometry for the $n - 1$ transverse directions). Thus, to walk away from an equilibrium molecular structure toward a transition state along the softest[14] (smallest b_a) distortion mode, one chooses λ in $b_1 < \lambda < {}^1/_2 b_2$ subject to $\mathbf{X}\cdot\mathbf{X} = h^2 = \sum_a [F_a^2/(\lambda - b_a)^2]$. As one approaches the desired transition state, the soft-mode local-Hessian eigenvalue b_1 becomes negative. From this point on, the NR step may be acceptable if $\mathbf{X}_{NR}\cdot\mathbf{X}_{NR} \leq h^2$; that is, if the step length constraint is unnecessary (for example, if the range of validity of the local quadratic energy approximation of eq 3 contains the transition-state geometry), the NR step is realistic and should be taken.

Once a transition state has been reached, one can walk "downhill" to product-molecule geometries by employing the same walking algorithm but with $\lambda < b_1$ so that the predicted energy change of eq 3 is negative along all n directions. At the start of such a downhill walk $b_1 < 0$, but as the product molecule's geometry is approached, b_1 becomes positive. Once this occurs, the NR step is again acceptable if its length is less than the specified maximum step length h.

The reaction path walking algorithm outlined above was successfully applied to several two- and three-dimensional potential energy surfaces in ref 7. The reader is referred to that paper for further details.

Be + H_2 Reaction Paths

Electronic Wave Function Characteristics. The contracted Gaussian-type orbital (GTO) basis set described in Table I was

(14) In ref 7 it is shown how one can also walk uphill in stream beds which lie along other (b_2, b_3, etc.) local-eigenmode directions by simply scaling the displacement coordinate (e.g., $X_2 = \alpha X_2'$) along the uphill walking direction. As a result of this scaling, the Hessian eigenvalue spectrum is changed so that the uphill walking direction can be made (by changing α) the softest mode (e.g., ${}^1/_2 X_2^2 b_2 = {}^1/_2(X_2')(\alpha^2 b_2)$).

utilized in all of the ab initio calculations reported here. This basis is identical with that employed by Banerjee et al.[16] in their coupled-cluster investigations into the electronic structure of $^1A_1$ BeH_2 and by Bartlett et al.[15] in their coupled-cluster study of the Be + H_2 → BeH_2 reaction.

The three asymptotic channels considered here (Be + H_2, BeH_2, and Be + 2H) require, as chemically essential electronic configurations, the following orbital occupancies (all orbital labels refer to C_{2v} symmetry):

$$\text{Be} + \text{H}_2; \quad 1a_1^2 2a_1^2 3a_1^2 \simeq 1s_{Be}^2\, 2s_{Be}^2\, 1\sigma_{g,H_2}^2$$

$$\text{BeH}_2; \quad 1a_1^2 2a_1^2 1b_2^2 \simeq 1s_{Be}^2 \sigma_{BeH}^2 \sigma'^2_{BeH}$$

$$\text{Be} + 2\text{H}; \quad 1a_1^2 2a_1^2 3a_1^2,\ 1a_1^2 2a_1^2 1b_2^2 \simeq 1s_{Be}^2 2s_{Be}^2 1\sigma_{g,H_2}^2,\ 1s_{Be}^2 2s_{Be}^2 1\sigma_{u,H_2}^2$$

Of course, the physical nature of the $1a_1$, $2a_1$, $3a_1$, and $1b_2$ orbitals vary throughout the potential energy surface. For example, the $1b_2$ orbital is a Be–H σ bonding orbital at the linear H–Be–H geometry, whereas it is an antisymmetric combination of two H 1s orbitals at the Be + 2H geometry. Likewise, $2a_1$ can be a Be–H σ bond or a Be 2s orbital. Because of these facts, we have chosen to use a multiconfiguration self-consistent field (MCSCF) wave function[17] for obtaining our ab initio energies, gradients, and Hessians. In particular, we used the simplest chemically reasonable MCSCF wave function consisting of the above two configurations ($1a_1^2 2a_1^2 3a_1^2$ and $1a_1^2 2a_1^2 1b_2^2$) in which the $1a_1$, $2a_1$, $3a_1$, and $1b_2$ orbitals are optimized at each geometry. Although this MCSCF wave function does contain the chemically essential configurations, it does not allow electron correlation effects to be properly treated. These effects would require, for example, Be $2p^2_{x,y,z}$ and H_2 σ_u^2 orbital occupancies not all of which are included in our two-configuration wave function. As a result, our MCSCF potential energy surface is probably qualitatively correct but not of high precision. Nevertheless, the primary motivation for this work was to examine the performance of the walking algorithm of ref 7 within an ab initio surface framework. This can certainly be achieved even with our two-configuration wave function.

Results of Stream Bed Walks. The starting geometries used in generating the stream bed walks are two different geometries of the BeH_2 "super molecule": the linear equilibrium BeH_2 geometry and a geometry corresponding to a Be atom 6.0 bohrs away from an equilibrium H_2 molecule. At each of these starting geometries, the forces and curvatures are calculated by a finite difference grid of seven points in the two-dimensional (R_{HH}, R_{Be-H_2}) coordinate space. From the initial forces and curvatures, a new geometry is then predicted by using the algorithm described earlier and, at that new point, the new energy and forces are calculated by a three-point finite difference grid. The Hessian is then updated by using the appropriate update method (i.e., the so-called BFGS method for downhill walks and the Powell method for transition-state walks (see ref 7 and 11 for definitions of the update procedures)) using the step vector and the change in the force vector. This new Hessian then allows the walking process to be continued in like fashion.

Calculating forces by such finite difference methods causes some difficulties in the resultant walks. Near the transition state, the slopes in the surface are so small that the finite difference-calculated forces do not seem to be sufficiently precise. Lack of precision in the converged MCSCF energies used to generate the finite difference forces is probably the cause. When such forces are used to update the Hessian, both the Hessian and the force vector contain spurious information. As a result, the walking algorithm may lead to unrealistic step predictions. By utilizing more accurate calculation methods (e.g. ab initio analytical gradient and Hessian expressions), this problem can be eliminated.

(15) G. D. Purvis and R. J. Bartlett, *J. Chem. Phys.*, **76**, 1910 (1982); G. D. Purvis, R. Shepard, F. Brown, and R. J. Bartlett, *Int. J. Quantum Chem.*, **23**, 835 (1983).
(16) A. Banerjee and J. Simons, submitted for publication in *Chem. Phys.*
(17) R. Shepard, I. Shavitt, and J. Simons, *J. Chem. Phys.*, **76**, 543 (1982).

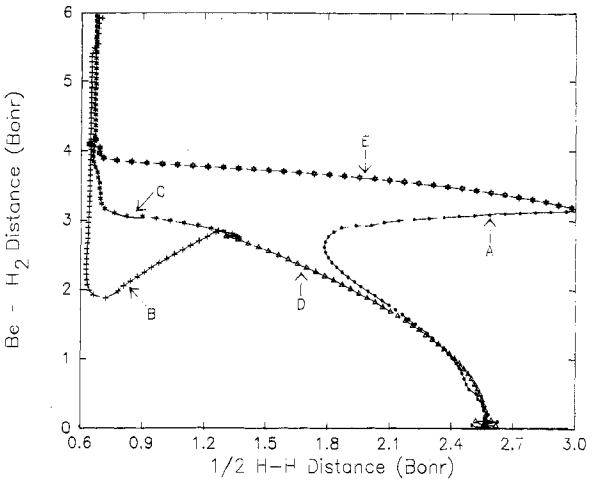

Figure 1. Walks on the BeH_2 surface (see text).

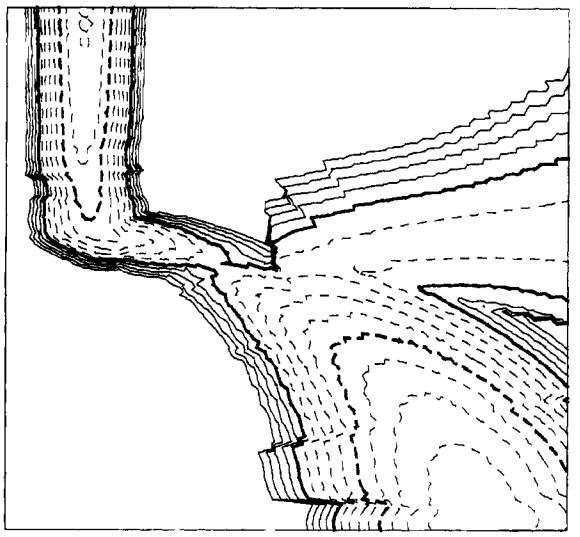

Figure 2. Contour view of the BeH_2 surface constructed by using only local forces and curvatures from walks A, C, and D in Figure 1.

TABLE II: Structural Information for the BeH_2 Surface

dist, bohrs		curvature, hartree/bohr^2		tot energy, hartrees
Be–H_2	$^1/_2$H–H,	Be–H_2	H–H	
0.00	2.54	0.037 211	0.328 224	−15.748 39
6.00	0.70	0.022 774	1.490 284	−15.714 41
2.85	1.27	0.144 974	−0.203 214	−15.544 51[a]
3.14	3.03	0.001 343	0.007 846	−15.562 36

[a] The curvatures at the transition state correspond to one imaginary frequency of 1.09×10^{15} s^{-1} and one real frequency of 8.55×10^{14} s^{-1}.

The first walk (A) depicted in Figure 1 moves uphill from the linear BeH_2 geometry. It starts by decreasing the H–H distance while pulling the Be atom out from between the hydrogen atoms. At a Be–H_2 distance of about 1.8 bohrs, the walk changes direction and begins to increase the H–H distance, finally leading to three separate atoms (still maintaining the C_{2v} symmetry). The slopes along both geometrical directions gradually approach zero, but no transition state is reached as no new bonds are being formed in BeH_2 → Be + 2H; this reaction is simply a double-bond-breaking reaction.

The second uphill walk (B) of Figure 1 starts from the Be + H_2 geometry and reaches a transition state located at (1.2657, 2.8514). A downhill walk from the transition state back to the same Be + H_2 geometry gives a more direct path (C). The fact that the uphill and downhill walks connecting these same two geometries are not coincident indicates that the walking algorithm is having some difficulty following the "stream bed". In this

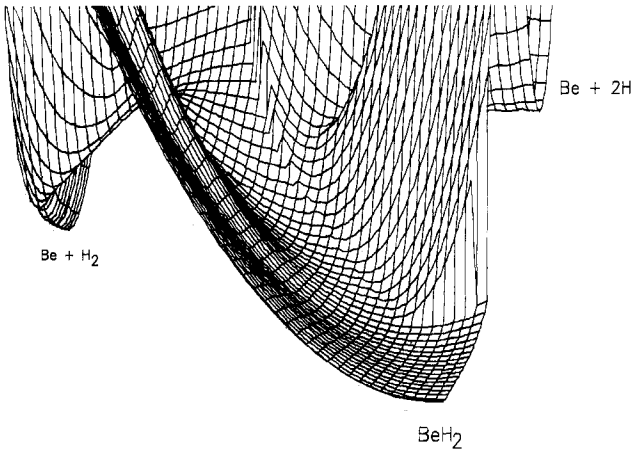

Figure 3. Hidden-line view of surface described in Figure 2.

particular case, it is likely that the problem arises because the surface is quite flat along the R_{Be-H_2} coordinate in the initial phase of the uphill Be + H_2 walk.

Path D represents a downhill walk from the transition state to the linear product BeH_2. This walk might, in principle, have been expected to possibly dissociate to Be + H + H. However, this is improbable because the algorithm is instructed to move downhill in all directions. Once the neighborhood of the stream bifurcation is reached, the Be + H + H products lie uphill.

Finally, path E of Figure 1 describes the downhill motion from Be + 2H to Be + H_2, which is, of course, nothing but the 2H → H_2 recombination reaction. This path does not go through a transition state because, as was the case in walk A, it describes a simple bond formation reaction, not a concerted breaking–formed reaction.

At each point on the above reaction paths, the information available includes the electronic energy and the forces and curvatures along and perpendicular to the reaction path. This *local* information can be used to construct an approximation to the C_{2v} potential energy surface (Figures 2 and 3) from which one can obtain a clear picture of the energetics of these reactions. The energetic and structural information needed to characterize the various reactant and transition-state species is summarized in Table II.

In summary, we see that the potential energy surface walking algorithm of ref 7 can reliably use only local force and curvature data to generate reaction paths, find transition states, and locate various product species. The extension of this method to permit more efficient location of reaction path bifurcations and to allow its use within dynamical studies cast in the language of ref 9 is currently under investigation.

Acknowledgment. We acknowledge the financial support of the National Science Foundation (Grant No. 8206845) and the donors of the Petroleum Research Fund, administered by the American Chemical Society.

Registry No. Be, 7440-41-7; H_2, 1333-74-0; BeH_2, 7787-52-2.

A Theoretical Study of Monosubstituted Allyl Cations

M. H. Lien

Department of Chemistry, National Chung-Hsing University, Taichung, Taiwan 400, Republic of China

and A. C. Hopkinson*

Department of Chemistry, York University, Downsview, Ontario, Canada M3J 1P3
(Received: August 12, 1983)

Ab initio molecular orbital calculations are reported for trans 1-X-allyl, cis 1-X-allyl, 2-X-allyl, and α-X-cyclopropyl cations, where X is H, CH_3, NH_2, OH, F, NC, and CN. Geometries were optimized by using a 3-21G basis set, and single-point calculations were done at the 6-31G* level. The stabilizing effects of the substituents are compared with the effect of the same substituents in the methyl cations. Substituents at the 2-position are found to have little effect on the barrier to rotation of a CH_2 group. Substituents at the 1-position raise the barrier to rotation of the CH_2 group while the barrier to rotation of the CHX group is lower than in the allyl cation.

Introduction

Allyl cations were first postulated as reaction intermediates and subsequently were directly observed in strong acid solutions.[1] The parent allyl cation is a well-characterized species in the gas phase,[2-4] and recently the 2-hydroxyallyl cation has been shown to be a long-lived species in the gas phase.[5]

The parent allyl cation is the simplest π-delocalized carbenium ion and consequently has been the subject of many theoretical studies.[6-12] There have also been two minimal STO-3G basis set studies on substituted allyl cations, one studying the relative energies of 2-substituted allyl cations and the isomeric α-substituted cyclopropyl cations[13] and the other studying the effect

(1) For a review, see N. C. Deno in "Carbonium Ions", Vol II, G. A. Olah and P. v. R. Schleyer Eds. Wiley-Interscience, New York, 1972, Chapter 18.
(2) D. H. Aue and M. T. Bowers in "Gas Phase Ion Chemistry", Vol. II, M. T. Bowers Ed., Academic Press, New York, 1979, pp 1-52.
(3) F. P. Lossing, *Can. J. Chem.*, **49**, 356 (1971); **50**, 3973 (1972).
(4) M. T. Bowers, L. Shuying, P. Kemper, R. Stradling, H. Webb, D. H. Aue, J. R. Gilbert, and K. R. Jennings, *J. Am. Chem. Soc.*, **102**, 4830 (1980).
(5) M. W. E. M. van Tilborg, R. van Doorn, and N. M. M. Nibbering, *J. Am. Chem. Soc.*, **101**, 7617 (1979).
(6) D. T. Clark and D. R. Armstrong, *J. Chem. Soc. D*, 850 (1969).
(7) S. D. Peyerimhoff and R. J. Buenker, *J. Chem. Phys.*, **51**, 2528 (1969).
(8) N. C. Baird, *Tetrahedron*, **28**, 2355 (1972).
(9) H. Kollmar and H. O. Smith, *Theor. Chim. Acta*, **20**, 65 (1971).
(10) L. Radom, P. C. Hariharan, J. A. Pople, and P. v. R. Schleyer, *J. Am. Chem. Soc.*, **95**, 6531 (1973).
(11) P. Merlet, S. D. Peyerimhoff, R. J. Buenker, and S. Shih, *J. Am. Chem. Soc.*, **96**, 959 (1974).
(12) K. Raghavachari, R. A. Whiteside, J. A. Pople, and P. v. R. Schleyer, *J. Am. Chem. Soc.*, **103**, 5649 (1981).

0022-3654/84/2088-1513$01.50/0